Letter to the Editor

Ruptured aneurysm at the meatal loop of the posterior inferior cerebellar artery: a case description

Min Yang

Department of Medical Imaging, Luzhou People's Hospital, Luzhou, China

Correspondence to: Min Yang, MM. Department of Medical Imaging, Luzhou People's Hospital, No. 316 Section 2 Jiugu Avenue, Jangyang District, Luzhou 646000, China. Email: yangmin822@126.com.

Submitted Nov 26, 2023. Accepted for publication Mar 27, 2024. Published online Apr 22, 2024.
doi: 10.21037/qims-23-1686
View this article at: https://dx.doi.org/10.21037/qims-23-1686

Introduction

Aneurysms of the posterior fossa reportedly account for 8–12% of all intracranial aneurysms (1). The posterior inferior cerebellar artery (PICA) aneurysms are relatively rare, the incidence has been reported as 0.5–3% (2). Intracanalicular aneurysms originating from the anterior inferior cerebellar artery (AICA) loop and unusual aneurysms located in the AICA-PICA variant have also been reported (3,4). Conventionally, these lesions present because of subarachnoid haemorrhage (SAH) combined with cranial nerve dysfunction (3). Ruptured intracanalicular PICA aneurysms have not been reported to date. Little is known about the features of aneurysms at the meatal loop of the PICA. Here, we report a case of ruptured PICA aneurysm at the top of the meatal loop.

Case presentation

All procedures performed in this study were in accordance with the ethical standards of the Institutional Review Board of the Luzhou People's Hospital, Luzhou and the Helsinki Declaration (as revised in 2013). Written informed consent was obtained from the patient for publication of this article and accompanying images. A copy of the written consent is available for review by the editorial office of this journal.

A 75-year-old woman visited the emergency department owing to a sudden onset of severe headache, dizziness, and hearing loss (Hunt and Hess Grade II). She had a history of high blood pressure; the highest systolic blood pressure was approximately 210 mmHg and her blood pressure control was not ideal. A brain computed tomography (CT) displayed a small high-density area in the left cerebellopontine angle (CPA) (*Figure 1*), which was compatible with SAH. Magnetic resonance imaging (MRI) showed SAH of the left CPA and internal auditory canal (IAC) (*Figure 2A,2B*). Three-dimensional time-of-flight (3D-TOF) (*Figure 3A,3B*) and minimum intensity projection (MIP) (*Figure 4A,4B*) with magnetic resonance angiography (MRA) showed that the left PICA formed a vascular loop in the IAC. Based on the Chavda classification, this vascular loop was classified as Type III. A small aneurysm was found at the top of left PICA meatal loop. Subsequently, computed tomography angiography (CTA) was performed and axial, MIP, and volume rendering (VR) (*Figure 5A,5B*) images were captured; however, these failed to fully expose the aneurysm in the left IAC owing to the artifacts from adjacent bone structures. On the fourth day after haemorrhage, a digital subtraction angiogram (DSA) demonstrated a 2-mm saccular aneurysm arising from the left PICA at the top of the meatal loop (*Figure 6*). The patient and her family refused surgical treatment. After 2 weeks of conservative treatment, including management of blood pressure, the headache and dizziness experienced by the patient had significantly improved (Hunt and Hess Grade I), and her hearing had partially recovered.

Discussion

The PICA is located at the lower part of the CPA; it shows a high frequency of variations, including hypoplastic, unilateral or bilateral absence, duplication, double origin, fenestration, vertebral artery terminating, location of the origin variation, and AICA-PICA common trunk variant (5). The PICA is adjacent to the medulla and the lower cranial nerves, making it difficult for a vascular loop to form in the IAC. The IAC vascular loop is mostly formed by the AICA and is referred to as the meatal loop (6). As reported previously, 14–40% of the AICA loops are in the meatus (7). The Chavda classification system classifies AICA loops into three types based on the location of the vascular loop relative to the IAC: Type I, the vascular loop lies in the CPA but does not enter into the IAC; Type II, the vascular loop enters the IAC but does not extend to 50% of the depth of the IAC; and Type III, the vascular loop extends 50% into the depth of the IAC (8) (*Figure 1*). Ruptured intracanalicular aneurysms at the vascular loop at the top of the PICA have not yet been reported.

Figure 1 CT image shows SAH in the left CPA. CT, computed tomography; SAH, subarachnoid haemorrhage; CPA, cerebellopontine angle.

Intracanalicular aneurysms, also referred to as intrameatal aneurysms, are characterized based on the location of the entire aneurysm within the IAC. Therefore, differential diagnosis between tumours and aneurysms may be difficult (9,10). Irrespective of whether the vascular loops originate from the AICA or PICA, intracanalicular aneurysms are always located at the top of vascular loops, such as in the present case; this may be caused by the high local impact force of blood flow. If ruptured, intracanalicular aneurysms cause SAH in the IAC and is likely to be accompanied with damage to the 7th and 8th cranial nerves. The patient in our report exhibited SAH in the IAC and CPA, accompanied by the involvement of the left 8th cranial nerve. The facial palsy, which is occasionally encountered, is the only sign in some cases to indicate such a rare lesion (7). The patient in this case study did

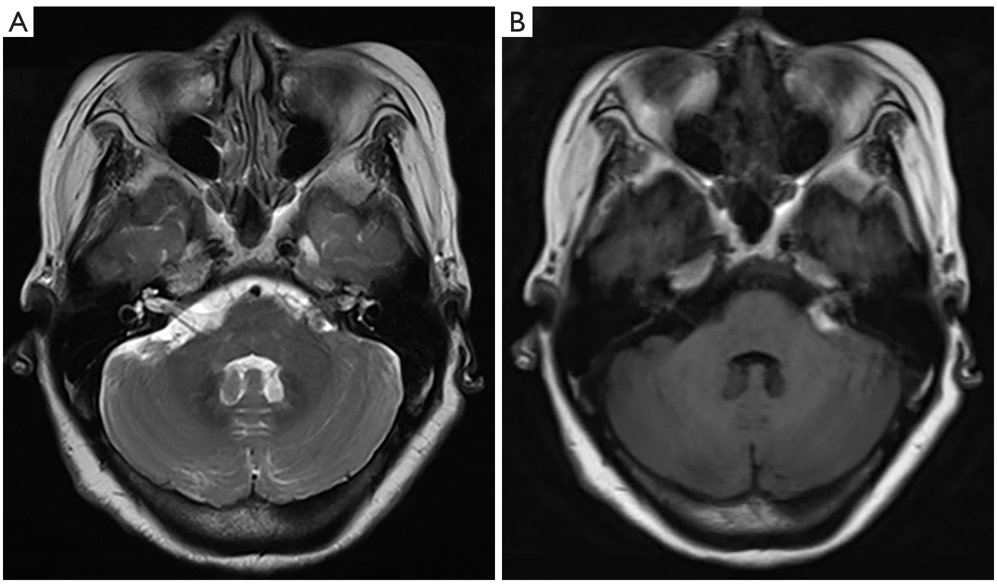

Figure 2 T2WI (A) and T1WI (B) images. (A) Heterogeneous signal intensity in the left CPA and slightly lower signal intensity in the IAC. (B) High signal intensity in the left CPA and IAC. T2WI, T2 weighted imaging; T1WI, T1 weighted imaging; CPA, cerebellopontine angle; IAC, internal auditory canal.

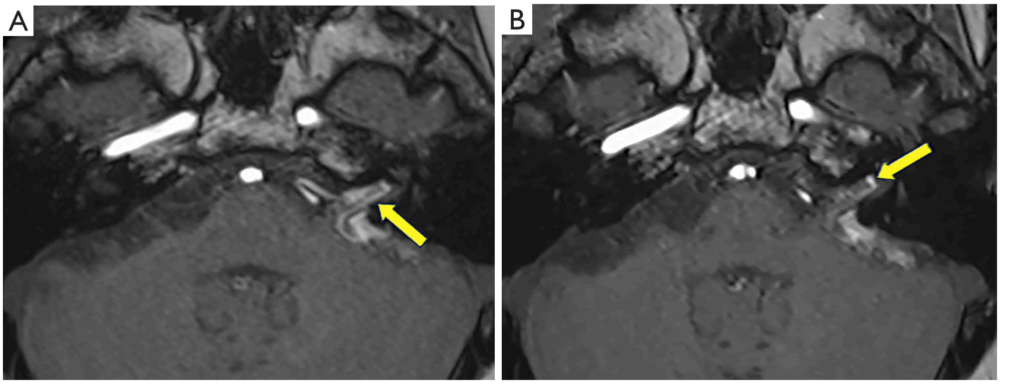

Figure 3 MRA 3D-TOF images. (A) High signal intensity in the left CPA and IAC, with a vascular loop (yellow arrow) in the IAC. (B) A small high signal aneurysm in the IAC (yellow arrow). MRA, magnetic resonance angiography; 3D-TOF, three-dimensional time-of-flight; CPA, cerebellopontine angle; IAC, internal auditory canal.

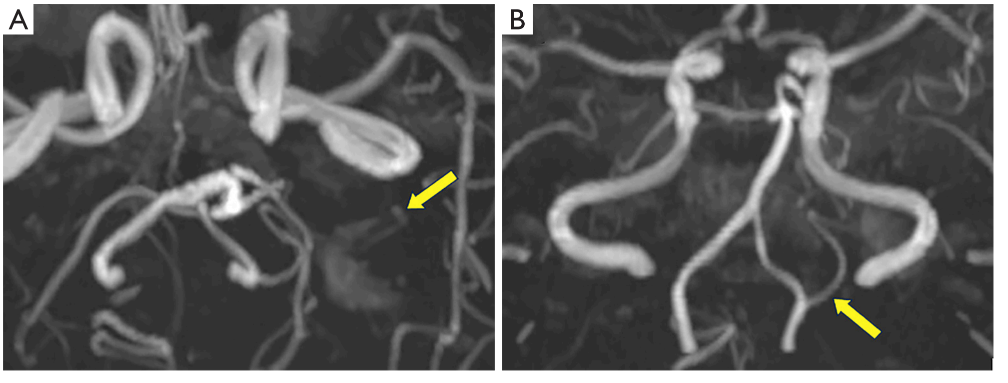

Figure 4 MRA MIP images. (A) The loop formed by the left PICA, with a small aneurysm (yellow arrow) at the top. (B) That the left PICA originates from the intracranial segment of the left vertebral artery (yellow arrow). MRA, magnetic resonance angiography; MIP, minimum intensity projection; PICA, posterior inferior cerebellar artery.

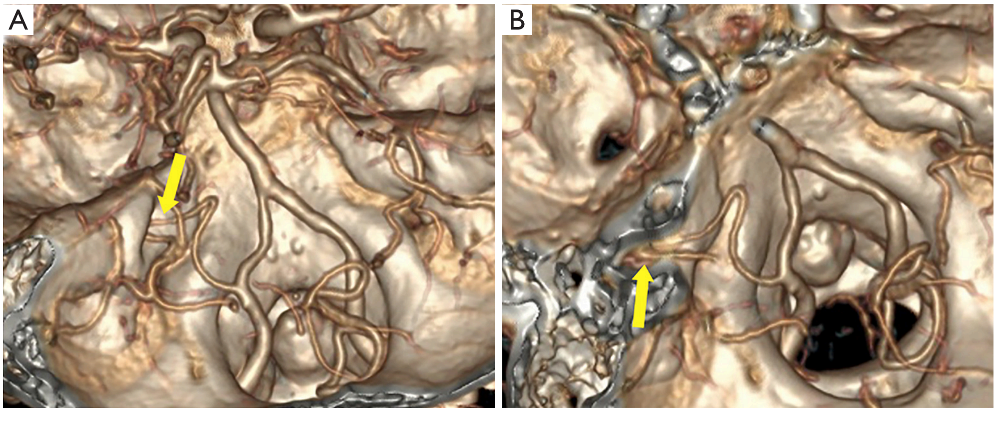

Figure 5 VR images. (A) The loop formed by the left PICA in the IAC (yellow arrow). (B) The aneurysm at the top of the vascular loop is obstructed by adjacent bone structures (yellow arrow). VR, volume rendering; PICA, posterior inferior cerebellar artery; IAC, internal auditory canal.

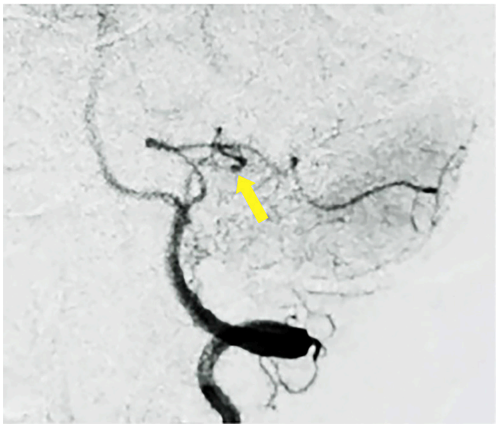

Figure 6 DSA image shows the loop formed by the left PICA, with a small aneurysm (yellow arrow) at the top. DSA, digital subtraction angiogram; PICA, posterior inferior cerebellar artery.

not present with any symptoms related to the facial nerves. After treatment, most patients with intracanalicular aneurysms will experience neuropathy, such as hearing loss (11). Regardless of the existence of a preoperative hearing impairment, the deeper the location of the aneurysm is in the IAC, the more serious the postoperative hearing impairment persists (1).

Clear display of the relationship of the aneurysm and adjacent bone structures is vital in treatment plan for patients with symptoms (12). Because MRA is not affected by the bone structures at the base of the skull, it can better show the intracanalicular aneurysms. In this case, the aneurysm in the IAC was first detected using MRA. The subsequent CTA did not show the lesions in a satisfactory manner compared with MRA images, primarily because of the artifacts of adjacent bone structures. These findings agree with previous reports in the literature (13). Although Jayaraman *et al.* thought that the high spatial resolution of axial CTA can effectively display these lesions (12), they cannot intuitively display aneurysm on tortuous arteries (14). Due to the inherent technical characteristics of MIP, any MIP image with a slab thickness greater than the thickness of the IAC would include contiguous bone in the voxel (12). Therefore, the density of the IAC bone is higher than the vascular vessel and would make the aneurysm displayed unclearly (12). On VR images, the vascular vessels are easily covered by the skull base bones, even if using subtraction and stripping software to separate vascular vessels from skull bone and other structures. Therefore, over-reliance on VR images remains the main reason of misdiagnosis (14). Due to the many advantages of CTA, it is still the main means in the initial diagnosis and evaluation of intracranial aneurysms (15). With two-dimensional (2D) DSA, the bone is subtracted by mask technique; however, the accurate position of IAC relative to the aneurysms is difficult to determine (12). The multi-planar reformation (MPR) technology of three-dimensional (3D) DSA can stretch and project images along the direction of the blood vessel diameter to observe the relationship with surrounding tissue structures. Therefore, 3D DSA is still considered the gold standard for diagnosis in this field (15).

Because of the relatively fragile wall, PICA aneurysms are prone to rupture even small in size (16). The death rate derived from recurrent bleeding in 48 hours of ruptured PICA aneurysms is three times higher than anterior circulation aneurysms (17). Patients with ruptured PICA aneurysms have a higher risk of nosocomial pneumonia and longer hospital stays in the intensive care unit (ICU) (18). When treating intracanalicular aneurysms, exposing and decompressing of all structures in the IAC, careful handling of the nerves and blood vessels, temporary trapping of the aneurysm, and careful dissection of the neck to avoid partially clipping are important procedures to reduce the risks of postoperative nerves injury (19). Coil embolization may be a therapeutic alternative to conventional open surgery (20).

The vascular loop of the IAC primarily originates from the AICA and occasionally from the PICA. When a meatal loop is discovered, it should be carefully assessed for any accompanying aneurysms. AICA and PICA intracanalicular aneurysms have similar locations on the vascular loop, clinical manifestations, treatment strategies, and prognoses. Although residual cranial nerve paralysis often occurs after surgery or interventional treatment, early treatment is still of vital importance.

Acknowledgments

The author would like to thank Yi Li, a researcher from Southwest Medical University. He provided tremendous encouragement and help before writing the paper. The author would also like to thank Elsevier Company for their assistance in language editing.
Funding: None.

Footnote

Conflicts of Interest: The author has completed the ICMJE uniform disclosure form (available at https://qims.

amegroups.com/article/view/10.21037/qims-23-1686/coif). The author has no conflict of interest to declare.

Ethical Statement: The author is accountable for all aspects of the work in ensuring that questions related to the accuracy or integrity of any part of the work are appropriately investigated and resolved. All procedures performed in this study were in accordance with the ethical standards of the Institutional Review Board of the Luzhou People's Hospital, Luzhou and the Helsinki Declaration (as revised in 2013). Written informed consent was obtained from the patient for publication of this article and accompanying images. A copy of the written consent is available for review by the editorial office of this journal.

References

1. Yamakawa H, Hattori T, Tanigawara T, Sahashi Y, Ohkuma A. Intracanalicular aneurysm at the meatal loop of the distal anterior inferior cerebellar artery: a case report and review of the literature. Surg Neurol 2004;61:82-8; discussion 88.
2. Williamson RW, Wilson DA, Abla AA, McDougall CG, Nakaji P, Albuquerque FC, Spetzler RF. Clinical characteristics and long-term outcomes in patients with ruptured posterior inferior cerebellar artery aneurysms: a comparative analysis. J Neurosurg 2015;123:441-5.
3. Zotta DC, Stati G, De Paulis D, Galzio RJ. Intrameatal aneurysm of the anterior inferior cerebellar artery. J Clin Neurosci 2011;18:561-3.
4. Gopalakrishnan CV, Menon G, Nair S. Aneurysm of the anterior inferior cerebellar artery-posterior inferior cerebellar artery variant: two case reports and review of literature. Br J Neurosurg 2009;23:554-6.
5. Brungardt JG, Liebscher SC, Schropp KP. Malrotation Correction in the Adult Population. World J Surg 2021;45:141-7.
6. Päsler D, Baldauf J, Runge U, Schroeder HW. Intrameatal thrombosed anterior inferior cerebellar artery aneurysm mimicking a vestibular schwannoma. J Neurosurg 2011;114:1057-60.
7. Kamano S, Kirino T, Mizuno S. Intrameatal aneurysm. Neurochirurgia (Stuttg) 1986;29:28-30.
8. McDermott AL, Dutt SN, Irving RM, Pahor AL, Chavda SV. Anterior inferior cerebellar artery syndrome: fact or fiction. Clin Otolaryngol Allied Sci 2003;28:75-80.
9. Liu DD, Kurland DB, Ali A, Golfinos JG, Nossek E, Riina HA. Pial brainstem artery arteriovenous malformation with flow-related intracanalicular aneurysm masquerading as vestibular schwannoma: illustrative case. J Neurosurg Case Lessons 2022;4:CASE22208.
10. Su Y, Richard SA, Lan Z. Posterior Inferior Cerebellar Artery Aneurysm Shaped Like a "Calabash Gourd" and Mimicking a Tumor. World Neurosurg 2024;184:161-2.
11. Okumura Y, Sakaki T, Hirabayashi H, Shimomura T. Intrameatal aneurysm successfully treated by meatal loop trapping--case report. Neurol Med Chir (Tokyo) 1999;39:161-4.
12. Jayaraman MV, Mayo-Smith WW, Doberstein CE. Intracanalicular aneurysm of the anterior inferior cerebellar artery revealed by multi-detector CT angiography. AJNR Am J Neuroradiol 2003;24:1338-40.
13. Kouskouras C, Charitanti A, Giavroglou C, Foroglou N, Selviaridis P, Kontopoulos V, Dimitriadis AS. Intracranial aneurysms: evaluation using CTA and MRA. Correlation with DSA and intraoperative findings. Neuroradiology 2004;46:842-50.
14. Zhang Y, Sun S, Xu Q, Feng W, Chen H. Posterior Inferior Cerebellar Artery Aneurysm: Have You Ever Been Misdiagnosed? Acad Radiol 2018;25:1564-7.
15. Wang X, Benson JC, Jagadeesan B, McKinney A. Giant Cerebral Aneurysms: Comparing CTA, MRA, and Digital Subtraction Angiography Assessments. J Neuroimaging 2020;30:335-41.
16. Narducci A, Xu R, Vajkoczy P. Decision Making in Surgery for Nonsaccular Posterior Inferior Cerebellar Artery Aneurysms With Special Reference to Intraoperative Assessment of Collateral Blood Flow and Neurophysiological Function. Oper Neurosurg (Hagerstown) 2018;14:422-31.
17. Thompson BG, Brown RD Jr, Amin-Hanjani S, Broderick JP, Cockroft KM, Connolly ES Jr, Duckwiler GR, Harris CC, Howard VJ, Johnston SC, Meyers PM, Molyneux A, Ogilvy CS, Ringer AJ, Torner J; American Heart Association Stroke Council, Council on Cardiovascular and Stroke Nursing, and Council on Epidemiology and

Prevention; American Heart Association; American Stroke Association. Guidelines for the Management of Patients With Unruptured Intracranial Aneurysms: A Guideline for Healthcare Professionals From the American Heart Association/American Stroke Association. Stroke 2015;46:2368-400.
18. Al-khayat H, Al-Khayat H, Beshay J, Manner D, White J. Vertebral artery-posteroinferior cerebellar artery aneurysms: clinical and lower cranial nerve outcomes in 52 patients. Neurosurgery 2005;56:2-10; discussion 11.
19. Sun Y, Wrede KH, Chen Z, Bao Y, Ling F. Ruptured intrameatal AICA aneurysms--a report of two cases and review of the literature. Acta Neurochir (Wien) 2009;151:1525-30.
20. Goto S, Ohshima T, Yamamoto T, Nishihori M, Nishizawa T, Shimato S, Kato K. A case of ruptured intrameatal aneurysm successfully treated with coil embolization. Nagoya J Med Sci 2015;77:307-13.

Cite this article as: Yang M. Ruptured aneurysm at the meatal loop of the posterior inferior cerebellar artery: a case description. Quant Imaging Med Surg 2024. doi: 10.21037/qims-23-1686